Supplementary Figure 1, Meijer et al.

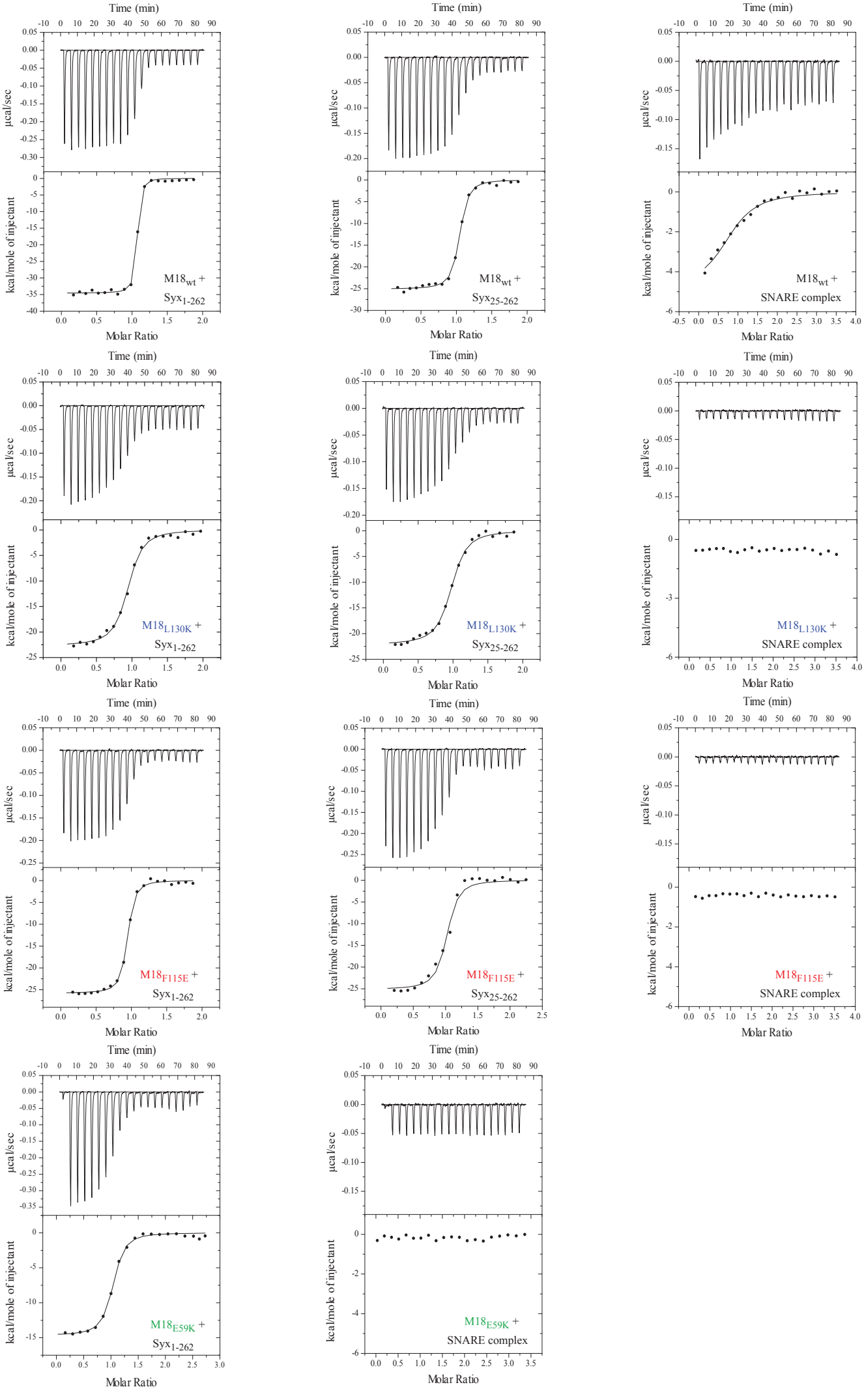

Figure S1. Isothermal titration calorimetry data for binding of Syntaxin1a to Munc18-1

All isothermal calorimetric experiments were performed at 25°C in PBS buffer, pH 7.4. In each titration, the Syntaxin1a variant or Syntaxin1a assembled into a purified ternary SNARE complex (as indicated) was injected into Munc18-1. In each figure, the top panel shows the base-line corrected raw data in power versus time during the injections. The lower panel displays the integrated areas normalized to the amount of injectant (kcal mol^{-1}) versus its molar ratio to Munc18-1. The solid lines represent the best fit to the data for a single binding site model using a nonlinear least squares fit. The results of the fits are given in Table 1. For experiments performed in replicate, a representative example is shown. The exact protein concentrations for the single ITC runs are: $M18_{WT}$ (2.5μM) + $Syx_{1\text{-}262}$ (20μM), $M18_{WT}$ (2.5μM) + $Syx_{25\text{-}262}$ (20μM), $M18_{WT}$ (4.0μM) + SNARE complex (60μM); $M18_{L130K}$ (2.5μM) + $Syx_{1\text{-}262}$ (20μM), $M18_{L130K}$ (2.5μM) + $Syx_{25\text{-}262}$ (20μM), $M18_{L130K}$ (4.0μM) + SNARE complex (60μM); $M18_{F115E}$ (2.5μM) + $Syx_{1\text{-}262}$ (20μM), $M18_{F115E}$ (2.5μM) + $Syx_{25\text{-}262}$ (20μM), $M18_{F115E}$ (4.0μM) + SNARE complex (60μM); $M18_{E59K}$ (4.0μM) + $Syx_{1\text{-}262}$ (57μM), $M18_{E59K}$ (4.0μM) + SNARE complex (60μM).

Supplementary Figure 2, Meijer et al.

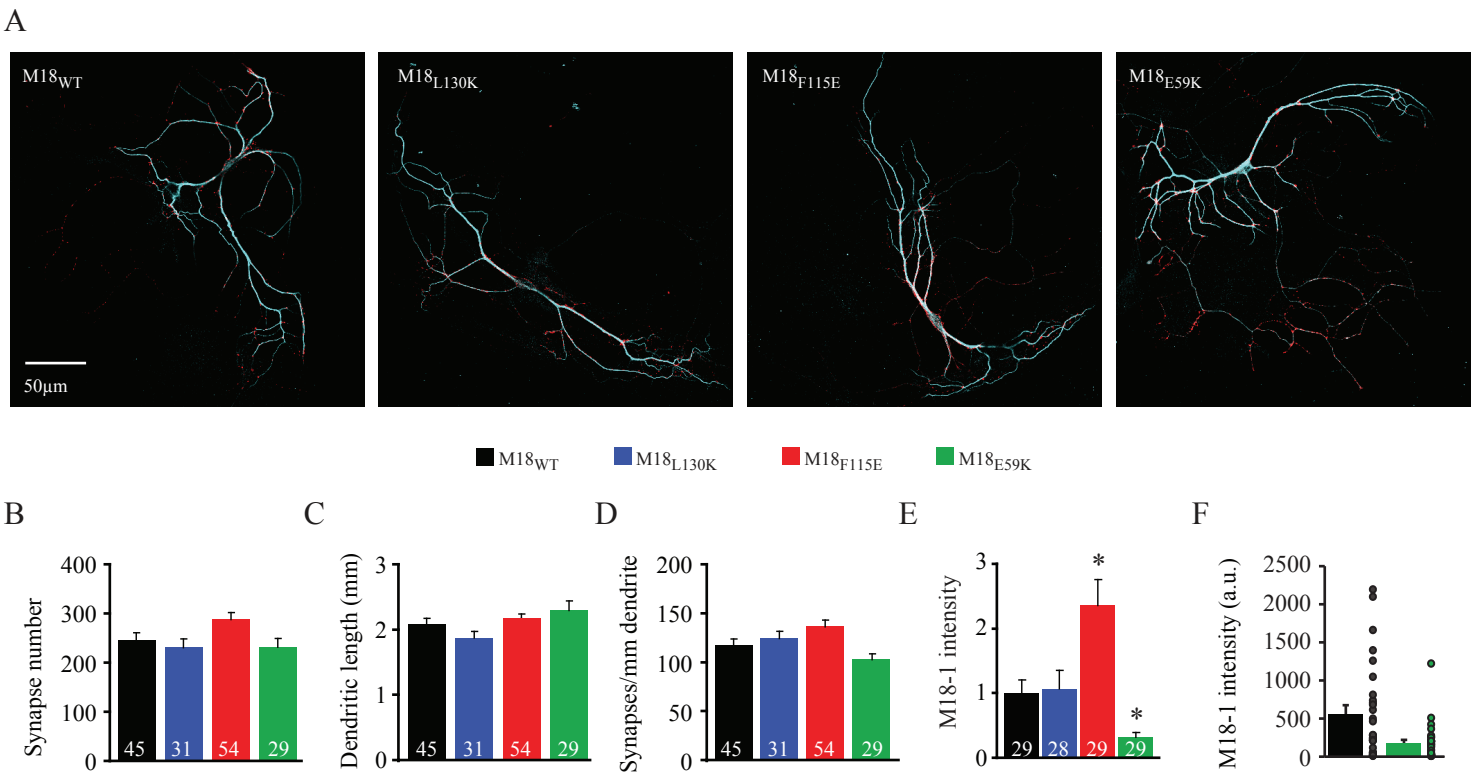

Figure S2. Neuronal morphology and synaptic protein levels.
(A) Representative images from *Munc18-1* null autaptic neurons rescued with $M18_{WT}$, $M18_{L130K}$, $M18_{F115E}$ or $M18_{E59K}$ and stained for MAP2 (blue) and VAMP (red). (B-D) The amount of synapses per neuron, dendritic length and synapse density were similar among groups. (E) Quantification of presynaptic protein levels from immuno-fluorescent confocal images in rescued *Munc18-1* null neurons (Kruskal-Wallis test with Dunn's post test, $P<0.05$ for $M18_{F115E}$ and $M18_{E59K}$). (F) Individual synaptic Munc18-1 levels per neuron, together with the mean value, are shown for $M18_{WT}$ and $M18_{E59K}$.

Data are mean ± SEM (significant differences from wt are depicted as *p < 0.05, **p<0.01, ***p<0.001).

Supplementary Figure 3, Meijer et al.

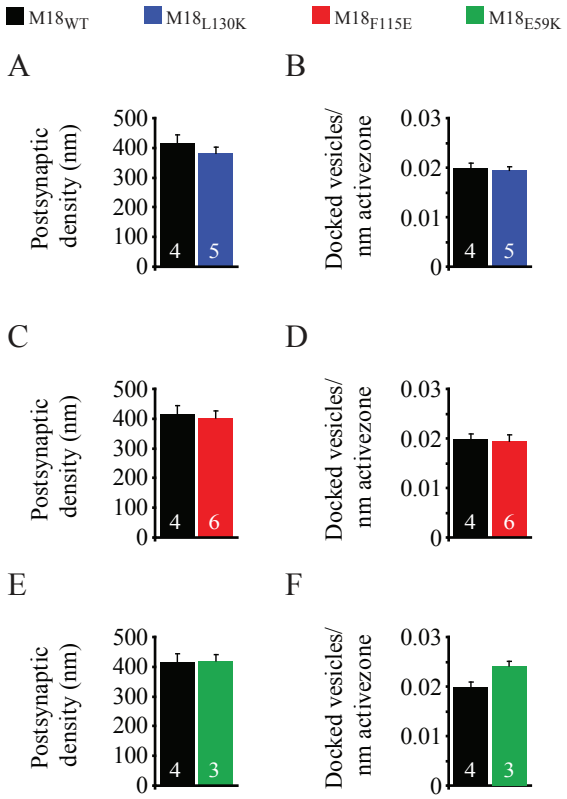

Figure S3. Ultrastructural features of the synapse by electron microscopy are normal
(A) The size of the postsynaptic density is normal in neurons rescued with $M18_{L130K}$. (B) Number of docked vesicles per nm active zone is normal in neurons rescued with $M18_{L130K}$. (C) The size of the postsynaptic density is normal in neurons rescued with $M18_{F115E}$. (D) Number of docked vesicles per nm active zone is normal in neurons rescued with $M18_{F115E}$. (E) The size of the postsynaptic density is normal in neurons rescued with $M18_{E59K}$. (F) Number of docked vesicles per nm active zone in neurons rescued with $M18_{E59K}$ is comparable to $M18_{WT}$.

N = 3-6 islands, n = 85-102 synapses. Data are mean ± SEM (significant differences from wt are depicted as *p < 0.05, **p<0.01, ***p<0.001).

Supplementary Figure 4, Meijer et al.

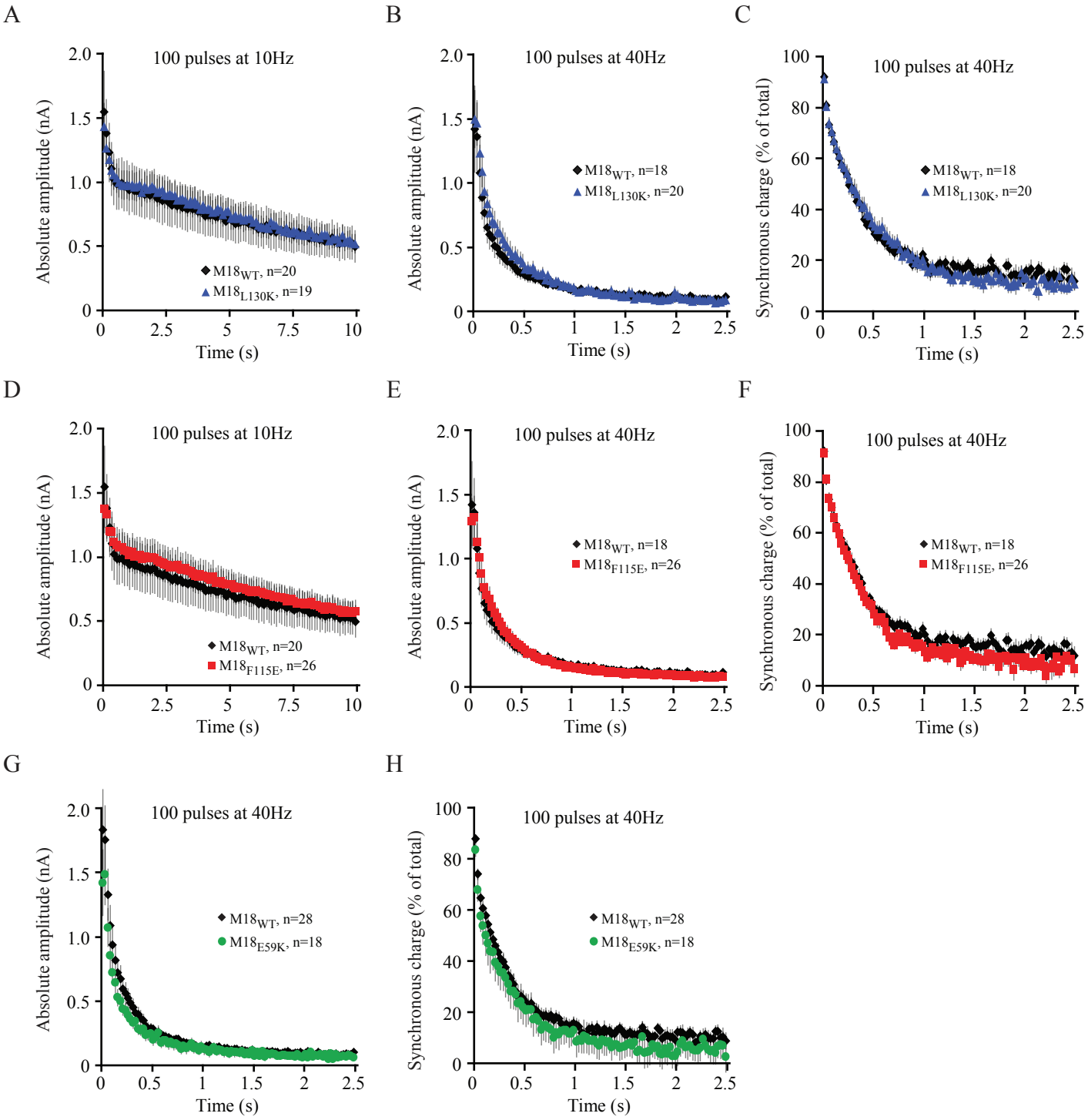

Figure S4. Rundown of EPSC sizes and synchronicity of release is unaltered during trains of stimulation. (A) EPSC sizes for $M18_{WT}$ and $M18_{L130K}$ during a train of 100 pulses at 10Hz. (B) EPSC sizes for $M18_{WT}$ and $M18_{L130K}$ during a train of 100 pulses at 40Hz. (C) Percentage of synchronous EPSC charge for $M18_{WT}$ and $M18_{L130K}$ in response to 100 pulses at 40Hz. (D) EPSC sizes for $M18_{WT}$ and $M18_{F115E}$ during a train of 100 pulses at 10Hz. (E) EPSC sizes for $M18_{WT}$ and M18 $M18_{F115E}$ during a train of 100 pulses at 40Hz. (F) Percentage of synchronous EPSC charge for $M18_{WT}$ and $M18_{F115E}$ in response to 100 pulses at 40Hz. (G) EPSC sizes for $M18_{WT}$ and $M18_{E59K}$ during a train of 100 pulses at 40Hz. (H) Percentage of synchronous EPSC charge for $M18_{WT}$ and $M18_{E59K}$ in response to 100 pulses at 40Hz.

Data are mean ± SEM.

Supplemental Figure 5, Meijer et al.

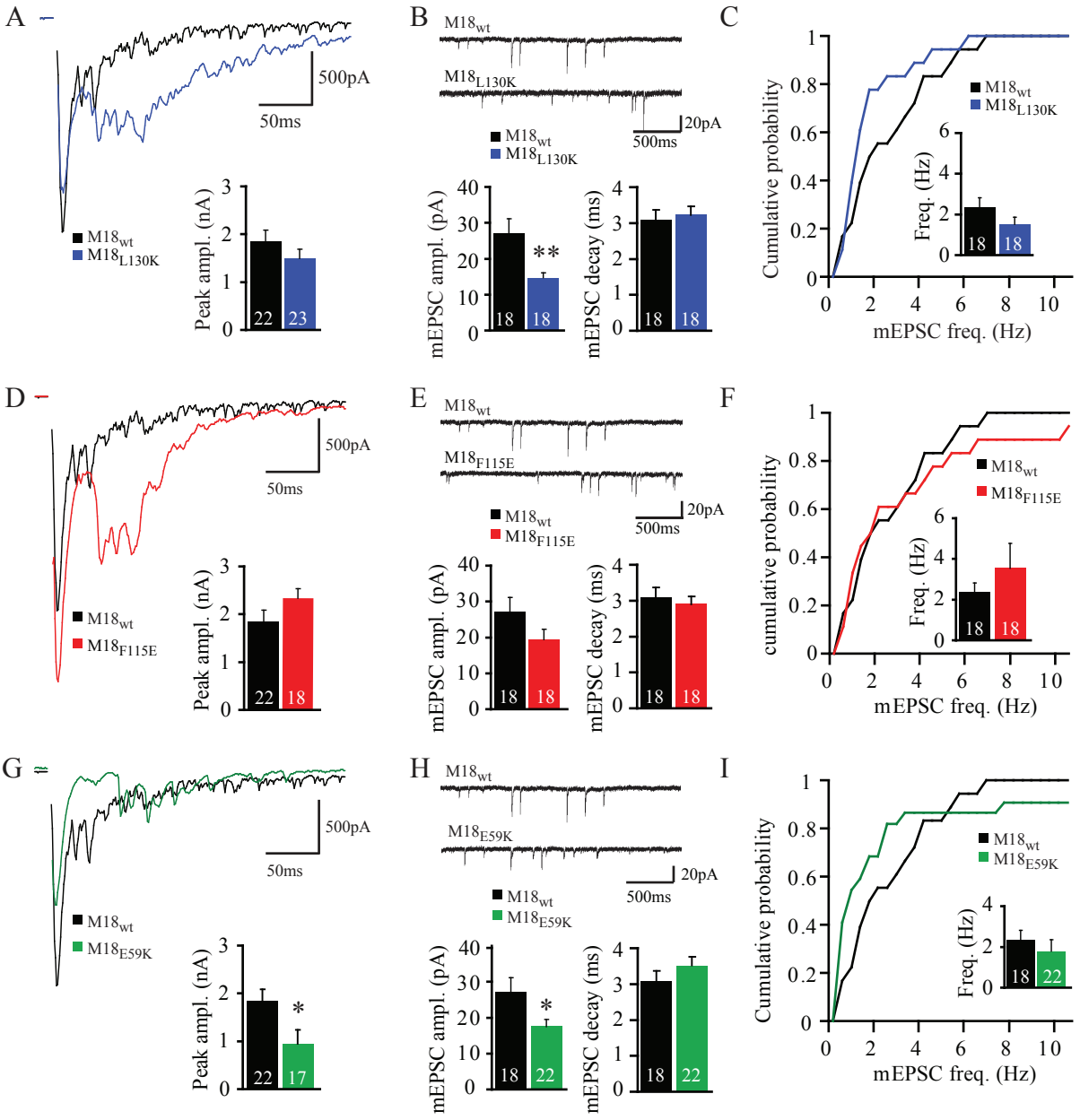

Figure S5. All mutants support synaptic transmission in network cultures

(A) Representative traces of field stimulation induced EPSCs in cortical cultures. Neurons rescued with $M18_{L130K}$ have a similar peak amplitude in response to field stimulation as neurons rescued with $M18_{WT}$. (B) Example traces of spontaneous release recorded in the presence of 1µM TTX. The amplitude of spontaneous release events is smaller in cultures rescued with $M18_{L130K}$ (Kruskal-Wallis with Dunn's post test, $P < 0.01$). The decay of the events is unchanged. (C) Cumulative frequency plot of spontaneous release events. Insert shows average frequency. (D) Representative traces of field stimulation induced EPSCs in cortical cultures. Neurons rescued with $M18_{F115E}$ have a similar peak amplitude in response to field stimulation as neurons rescued with $M18_{WT}$. (E) Example traces of spontaneous release recorded in the presence of 1µM TTX. The amplitude of spontaneous release events is unaffected. The decay of the events is unchanged. (F) Cumulative frequency plot of spontaneous release events. Insert shows average frequency. (G) Representative traces of field stimulation induced EPSCs in cortical cultures. Neurons rescued with $M18_{E59K}$ produce smaller peak amplitudes in response to field stimulation than neurons rescued with $M18_{WT}$ (ANOVA with Bonferroni post test, $P < 0.05$). (H) Example traces of spontaneous release recorded in the presence of 1µM TTX. The amplitude of spontaneous release events is smaller in neurons rescued with $M18_{E59K}$ (Kruskal-Wallis with Dunn's post test, $P < 0.05$). The decay of the events is unchanged. (I) Cumulative frequency plot of spontaneous release events. Insert shows average frequency.

Data are mean ± SEM (Significant differences from wt are depicted as *$p < 0.05$, **$p<0.01$, ***$p<0.001$).